Shallow impurity absorption spectroscopy in isotopically enriched silicon

M. Steger,[1] A. Yang,[1] D. Karaiskaj,[1] M. L. W. Thewalt,[1,*] E. E. Haller,[2] J. W. Ager III,[2] M. Cardona,[3] H. Riemann,[4] N. V. Abrosimov,[4] A. V. Gusev,[5] A. D. Bulanov,[5] A. K. Kaliteevskii,[6] O. N. Godisov,[6] P. Becker,[7] and H.-J. Pohl[8]

[1]*Department of Physics, Simon Fraser University, Burnaby, British Columbia, Canada V5A 1S6*

[2]*University of California Berkeley and LBNL, Berkeley, California 94720, USA*

[3]*Max-Planck-Institut für Festkörperforschung, 70569 Stuttgart, Germany*

[4]*Institut für Kristallzucht (IKZ), 12489 Berlin, Germany*

[5]*IChHPS of the RAS, 603000 Nizhny Novgorod, Russia*

[6]*Science and Technical Center "Centrotech," 198096 St. Petersburg, Russia*

[7]*Physikalisch-Technische Bundestanstalt Braunschweig, 38116 Braunschweig, Germany*

[8]*VITCON Projectconsult GmbH, 07743 Jena, Germany*

(Received 2 April 2009; published 20 May 2009)

Inhomogeneous broadening due to isotopic randomness in natural Si has been shown to cause a broadening of many of the ground-state to excited-state infrared-absorption transitions of the shallow donor phosphorus and acceptor boron. Previously, it had been thought that the observed linewidths of shallow impurity transitions in silicon were at their fundamental lifetime limit. We report improved high-resolution infrared-absorption studies of these transitions in new samples of isotopically enriched ^{28}Si, ^{29}Si, and ^{30}Si. Some of the transitions in ^{28}Si show the narrowest linewidths ever reported for shallow donor and acceptor absorption transitions, and many higher excited states are now observed. The improved samples of ^{29}Si and ^{30}Si result in revised values for the dependence of shallow donor and acceptor binding energies on the average Si mass.

DOI: 10.1103/PhysRevB.79.205210 PACS number(s): 71.55.Cn, 78.30.Am

I. INTRODUCTION

Most of the works on the effects of the isotopic composition of the host material on the optical and electronic properties of semiconductors have focused on effects controlled by the average composition.[1–3] More recently, high-quality crystals of isotopically pure Si have become available,[4,5] which reveal effects that are controlled not by the average composition but rather by the randomness of the composition present in crystals having the natural isotopic abundance.[6,7]

Karaiskaj *et al.*[7] showed that the isotopic randomness present in natural Si (^{nat}Si) causes a significant inhomogeneous broadening of many of the long-studied ground-state to excited-state infrared-absorption transitions of the shallow donor phosphorus and acceptor boron. This was surprising since it was thought that the observed linewidths of shallow impurities in silicon are at their fundamental lifetime limit.[8–10] Very recently, measurements of the excited-state lifetime for some of the absorption transitions in Si:P have been made which are in reasonable agreement with the reduced linewidths observed in ^{28}Si.[11]

Here we report on improved high-resolution infrared-absorption studies of the shallow impurities phosphorus and boron in new samples of isotopically enriched ^{28}Si, ^{29}Si, and ^{30}Si. These data improve on the linewidths of earlier spectra[7,12] particularly for the higher excited states due to reduced concentration broadening. Some of the transitions in ^{28}Si show the narrowest full width at half maximum (FWHM) ever reported for shallow donor and acceptor absorption transitions in semiconductors. In the case of boron the new samples also result in a significant increase in the number of observable absorption lines. With regard to the determination of the impurity-binding-energy shift with isotopic mass between ^{28}Si and ^{30}Si, the greatly improved spectra of the new ^{30}Si sample provide more accurate results than in our preliminary study.[12] A similar effect has been observed[13] previously for the B acceptor in ^{13}C vs ^{12}C diamond, and later explained[14] in terms of changes in the ground-state and excited-state binding energies due to a small dependence of the hole effective mass on the host isotopic composition. The shift in transition energies for both B and P between ^{30}Si and ^{28}Si has been explained by the same mechanism, with the inclusion of the dependence of the dielectric constant on the host isotopic composition.[12]

II. EXPERIMENTAL METHOD

The main improvement over our preliminary studies[7,12,15] was the improved quality of the samples used here, either in terms of the enrichment for ^{28}Si or in terms of the chemical purity and crystalline perfection for ^{29}Si and ^{30}Si. The ^{28}Si sample studied here was used before for photoluminescence excitation (PLE) experiments[16] and has an isotopic composition of 99.991% ^{28}Si+0.0075% ^{29}Si+0.0015% ^{30}Si. It also has an improved chemical purity and lighter doping levels with concentrations of $[P]=2\times10^{12}$ cm^{-3} and $[B]=5\times10^{13}$ cm^{-3}. For the boron spectra a sample with higher enrichment (99.995% ^{28}Si) was used, with a low phosphorus concentration of $[P]=5\times10^{11}$ cm^{-3} and boron concentration of $[B]=4.5\times10^{13}$ cm^{-3}.[17] The new ^{29}Si and ^{30}Si samples have a higher chemical purity but a lower isotopic enrichment, and the severe broadening and splitting[18,19] observed in the earlier samples are eliminated. The isotopic composition of the ^{29}Si sample is 4.32% ^{28}Si+91.37% ^{29}Si+4.30% ^{30}Si, with impurity concentrations of $[P]=2\times10^{13}$ cm^{-3} and $[B]=5\times10^{13}$ cm^{-3}, and for the ^{30}Si sample the enrichment

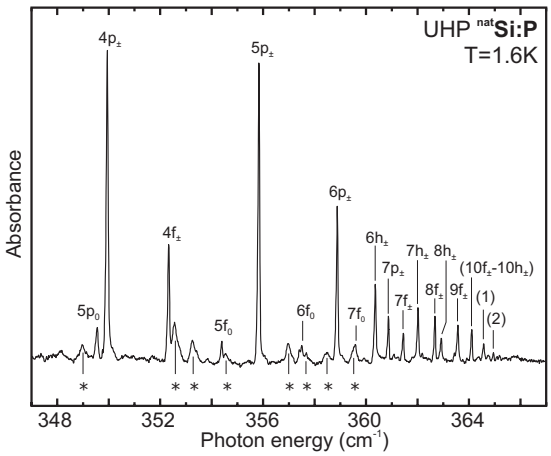

FIG. 1. High-energy end of the IR absorption spectrum of P-doped UHP ^{nat}Si at 1.6 K. Labels are assigned according to Pajot *et al.* (Ref. 24), no published data is available for lines (1) and (2). ∗ denotes absorption due to B.

is 2.50% ^{28}Si+7.70% ^{29}Si+89.80% ^{30}Si, with impurity concentrations of $[P]=2\times10^{13}$ cm^{-3} and $[B]=9\times10^{13}$ cm^{-3}. While the chemical purity of the enriched samples is improved, it still does not match that of ultrahigh-purity (UHP) natural silicon samples.

The samples were freely suspended in a sample chamber filled with superfluid He and sealed with polypropylene windows. The spectra were collected with a Bomem DA8.02 Fourier transform interferometer using either a silicon composite bolometer at 1.6 K or a Si:B photoconductive detector at 4.2 K, together with Mylar beamsplitters. For the high-resolution spectra a Globar source was used. To improve the spectra an additional quartz halogen source was used to illuminate the sample in order to achieve photoneutralization. The instrumental resolution for the phosphorus spectra was 0.012 cm^{-1}, and as low as 0.006 cm^{-1} for boron spectra, as verified by the observed linewidths of residual gas absorption lines. Samples with different thicknesses were used to obtain spectra covering the stronger transitions as well as the very weak higher-lying ones.

III. RESULTS AND DISCUSSION

A. Natural silicon

For the donor phosphorus in ^{nat}Si (Fig. 1) we report narrower lines and higher excited states than shown previously.[20–23] The $2p_0$ absorption line has a FWHM of 0.082 cm^{-1} and the $7p_\pm$ has a FWHM of only 0.057 cm^{-1}. All energies and linewidths are listed in Table I. Our sample also reveals two absorption lines for which we could not

TABLE I. Observed energies and FWHM of phosphorus absorption transitions in silicon. All energies in cm^{-1}.

	^{28}Si		^{nat}Si		^{29}Si	^{30}Si
	Energy	FWHM	Energy	FWHM	Energy	Energy
$2p_0$	275.090	0.033	275.108	0.082	275.128	275.147
$2p_\pm$	315.948	0.061	315.966	0.123	316.008	316.048
$3p_0$	323.436	0.135	323.460	0.166	323.499	323.541
$4p_0$	340.906	0.078	340.921	0.122	340.980	341.025
$3p_\pm$	342.429	0.051	342.449	0.105	342.492	342.540
$5p_0$	349.538		349.549	0.103	349.610	349.650
$4p_\pm$	349.924	0.029	349.952	0.089	349.990	350.037
$4f_\pm$	352.308	0.026	352.337	0.075	352.383	352.430
$5f_0$			354.401	0.092	354.443	354.480
$5p_\pm$	355.814	0.022	355.841	0.072	355.879	355.931
$6f_0$					357.511	357.555
$6p_\pm$	358.857	0.023	358.888	0.071	358.935	358.983
$7f_0$	359.550					
$6h_\pm$	360.345		360.366	0.069	360.431	360.478
$7p_\pm$	360.844		360.876	0.057	360.915	360.958
$7f_\pm$	361.427		361.453	0.069	361.506	361.555
$7h_\pm$	361.995		362.029	0.063	362.082	362.125
$8f_\pm$	362.662		362.683	0.058	362.730	362.794
$8h_\pm$	362.897		362.929	0.068	362.990	
$9f_\pm$	363.546		363.575	0.078	363.635	
$10f_\pm-10h_\pm$			364.113	0.059	364.170	
(a)			364.578	0.082		
(b)			364.957	0.057		

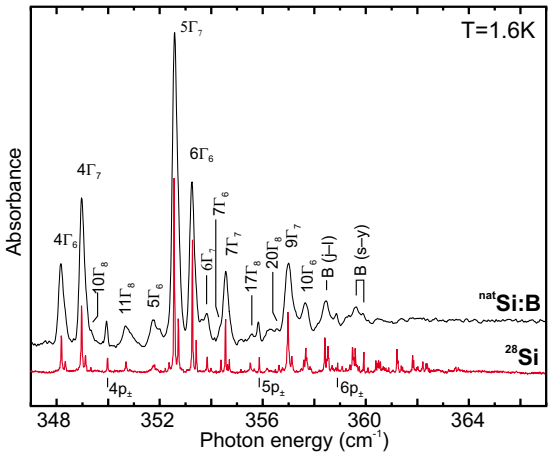

FIG. 2. (Color online) High-energy end of the IR absorption spectrum of B-doped ^{nat}Si and of ^{28}Si at 1.6 K. Labels are assigned according to Lewis *et al.* (Ref. 25). "a, b,…,aa, and ab,…" are used where no labels are available, and transitions due to P are labeled below the spectrum.

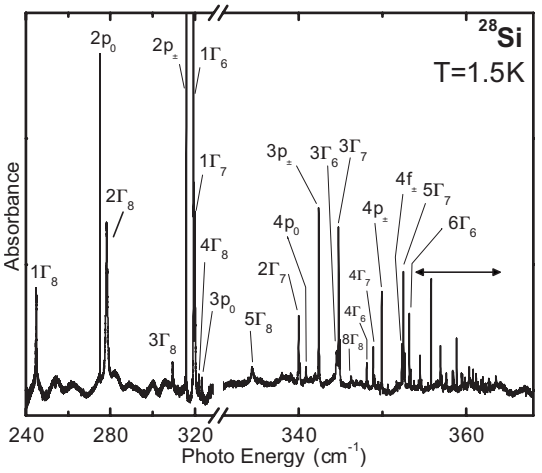

FIG. 3. Infrared-absorption spectrum of enriched, ultrapure ^{28}Si at 1.5 K. All major B and P absorption lines are labeled. The arrow indicates the range shown on an expanded scale in Fig. 4. The instrumental resolution is 0.02 cm^{-1}.

assign previously published final states and are therefore labeled (1) and (2). All other labels were assigned according to Pajot *et al.*[24]

We show a spectrum of the acceptor B in natural silicon in Fig. 2. Due to the high number of different labeling schemes we attempted to assign symmetry labels of theoretically calculated excited states wherever possible. These were given by Lewis *et al.*[25] where their energies are listed together with oscillator strength and compared to other labeling schemes.[26,27] Our spectrum clearly shows boron absorption lines up to the $9\Gamma_7$ [labeled (11) by Fischer and Rome[27]] and $10\Gamma_6$ transitions. Higher-energy lines that were verified to be B absorption transitions (by comparing to a ^{28}Si sample, see Fig. 2) but for which no final-state label was available were labeled with letters "a, b,…,aa, and ab,…."

B. Isotopically enriched ^{28}Si

Figure 3 shows a complete spectrum of a ^{28}Si sample containing both residual boron and phosphorus with all major lines labeled. The high-energy end of the spectrum is shown on an expanded scale in Fig. 4 due to the high density of transitions.

In previous publications[7] on isotopically enriched ^{28}Si only the low-energy absorption lines of the donor phosphorus were found to be sharper than in ^{nat}Si due to concentration broadening of higher-excited states. With the new higher-quality ^{28}Si material we can report narrower P and B absorption linewidths for many of the high-energy transitions as well. The phosphorus $5p_\pm$ line has a FWHM of 0.022 cm^{-1} (0.019 cm^{-1} correcting for the instrumental res-

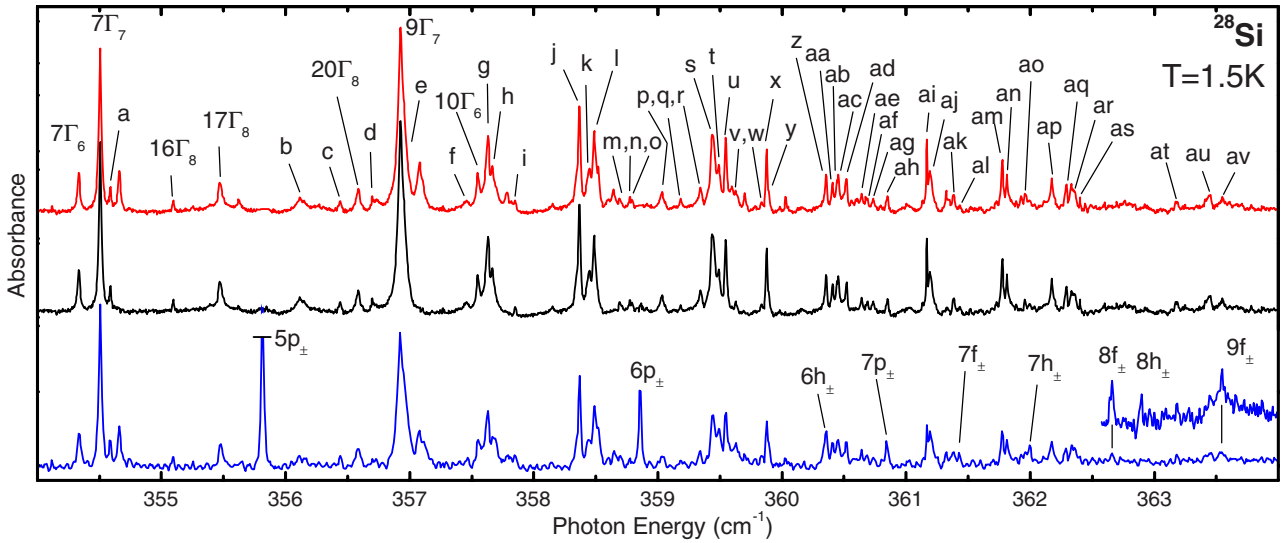

FIG. 4. (Color online) Infrared-absorption spectrum of enriched, ultrapure ^{28}Si at 1.5 K (high-energy end). The top two spectra are from a sample with low-P concentration. All identified ^{10}B-^{11}B pairs are labeled. The middle spectrum has all ^{10}B absorption lines removed synthetically. The instrumental resolution is 0.006 cm^{-1}. The bottom spectrum and inset show phosphorus absorption lines taken from two samples with higher residual P concentration, both at a resolution of 0.02 cm^{-1}.

olution of 0.012 cm^{-1}), five times narrower than that reported by Andreev *et al.*[23] and only two times wider than the narrowest absorption line reported for the deep center Se.[28] The use of samples with different residual P levels made it possible to identify weak high-energy P absorption lines up to the $9f_{\pm}$ transition, as shown at the bottom of Fig. 4. Table I shows the measured position and FWHM of phosphorus absorption lines in ^{28}Si, ^{nat}Si, ^{29}Si, and ^{30}Si.

Thanks to the reduction in concentration broadening we have observed narrower absorption lines for the acceptor boron as well. Most of the boron transitions reveal a $\sim 0.154 \pm 0.002$ cm^{-1} splitting in ^{28}Si which was attributed to the difference in binding energy between ^{10}B and ^{11}B acceptors.[7] The doublet intensity ratio reflects the ^{11}B/^{10}B natural abundance ratio of $\sim 80/20$. This characteristic doublet can be used to identify many high-energy B absorption transitions that have not been reported previously. For easier reference we attached new alphabetic labels "a, b,…,aa, and ab,…" to these lines. The observed linewidths for these higher-energy B transitions are even narrower than those of P.

The *p*-type character of the ^{28}Si sample makes it necessary to use photoneutralization in order to see the donor transitions. The photoneutralization also reduces electric fields due to ionized impurities, and thus reduces the inhomogeneous Stark broadening of both boron and phosphorus absorption lines. For a number of B lines we measure a FWHM in the range of 0.010–0.013 cm^{-1} (0.008–0.012 cm^{-1} corrected for the instrumental resolution). This is more than 20 times narrower than B transitions reported by Lewis *et al.*[25] for B in ^{nat}Si, and only about 1.5 times wider than the narrowest absorption line reported for the deep center Se.[28] The measured position and FWHM of B absorption lines in ^{28}Si, ^{nat}Si, ^{29}Si, and ^{30}Si are shown in Tables II and III. Figure 4 shows a spectrum of the high-energy end of boron absorption lines. We have also generated a spectrum that eliminates the ^{10}B components through a shift-and-subtract procedure to simplify the identification of many boron-related absorption features.

1. Isotope broadening

The broadening seen in ^{nat}Si or any sample of mixed isotopic composition is dominated by an effect[7] that is independent of the small shifts in binding energy between pure ^{28}Si, ^{29}Si, and ^{30}Si which will be discussed later. The wave function of the ground state is relatively compact; so in samples with mixed isotopes, individual impurities can have significantly different local isotopic compositions. These fluctuations induce shifts (and splittings for acceptors[29]) of the ground states, which can be related to the known shifts of valence-band and conduction-band energies with average isotopic composition. The excited-state wave functions are much more extended and therefore sample an isotopic composition closer to the average. The difference in isotopic composition sampled by excited-state and ground-state results in inhomogeneous broadening. The valence-band shifts more than the conduction band with the isotopic composition[7] causing a stronger broadening for the acceptor B than for the donor P.

TABLE II. Observed energies and FWHM of lower energy boron absorption transitions in silicon. For ^{28}Si the energies of the ^{11}B components are given, the transition energy of ^{10}B is 0.154 cm^{-1} higher. All energies in cm^{-1}. (Continued in Table III.)

Symmetry (Ref. 25)/label	^{28}Si (^{11}B)		^{nat}Si	^{29}Si	^{30}Si
	Energy	FWHM	Energy	Energy	Energy
$1\Gamma_8$	244.929	0.423	244.946	245.089	245.193
$2\Gamma_8$	278.260	0.839	278.295	278.443	278.571
$3\Gamma_8$	309.503	0.458	309.531	309.704	309.827
$1\Gamma_6$	319.335	0.094	319.374	319.535	319.687
$1\Gamma_7$	320.013	0.386	320.032	320.199	320.347
$4\Gamma_8$	321.887	0.339	321.910	322.106	322.254
$5\Gamma_8$	334.490	0.395	334.517	334.688	334.846
$2\Gamma_6$	338.032	0.419	338.042		
$6\Gamma_8$	339.080	0.130	339.151	339.336	
$2\Gamma_7$	340.025	0.064	340.045	340.264	340.407
$7\Gamma_8$	342.021	0.083			
$3\Gamma_6$	344.539	0.140	344.544	344.754	344.883
$3\Gamma_7$	344.783	0.041	344.834	345.012	345.164
$8\Gamma_8$	346.268	0.120	346.303	346.499	
$4\Gamma_6$	348.132	0.043	348.171	348.355	348.510
$4\Gamma_7$	348.918	0.042	348.982	349.162	349.330
$10\Gamma_8$	349.277	0.026			
$11\Gamma_8$	350.640	0.055	350.689		
$5\Gamma_6$	351.703	0.120	351.751		
$5\Gamma_7$	352.517	0.029	352.593	352.760	352.924
$6\Gamma_6$	353.221	0.024	353.259	353.448	353.605
$6\Gamma_7$	353.796	0.036	353.847		354.170
$7\Gamma_6$	354.332	0.028			
$7\Gamma_7$	354.507	0.025	354.574	354.748	
(a)	354.589	0.012			
$16\Gamma_8$	355.095	0.018			
$17\Gamma_8$	355.473	0.033	355.584		
(b)	356.110				
(c)	356.439				
(d)	356.699				
$20\Gamma_8$	356.585	0.049			
$9\Gamma_7$	356.925	0.044	357.005	357.178	
(e)	356.961	0.049			
(f)	357.458				
$10\Gamma_6$	357.549	0.036	357.662		
(g)	357.628	0.042			
(h)	357.668	0.019			
(i)	357.850	0.018			
(j)	358.367	0.024	358.470		

Lifetime broadening as a limiting factor for the width of absorption lines dominates for some transitions, hence their FWHM does not decrease significantly in isotopically enriched ^{28}Si. An example would be the $1\Gamma_7$ transition shown in Fig. 5 or $1\Gamma_8$ in Fig. 7. This lifetime broadening effect was explained by Kane[8] and confirmed by Barrie and

TABLE III. Observed energies and FWHM of high energy ^{11}B absorption transitions in ^{28}Si. All energies in cm^{-1}.

Label	Energy	FWHM	Label	Energy	FWHM
(k)	358.446	0.040	(ad)	360.520	0.015
(l)	358.487	0.027	(ae)	360.641	0.025
(m)	358.694	0.020	(af)	360.689	0.012
(n)	358.773	0.013	(ag)	360.735	0.029
(o)	358.792	0.015	(ah)	360.848	0.022
(p)	359.032	0.035	(ai)	361.167	0.010
(q)	359.184	0.019	(aj)	361.195	0.036
(r)	359.341	0.030	(ak)	361.382	0.023
(w)	359.442	0.043	(al)	361.434	
(t)	359.492	0.032	(am)	361.773	0.019
(u)	359.547	0.018	(an)	361.812	0.015
(v)	359.625		(ao)	361.957	0.012
(w)	359.835	0.017	(ap)	362.173	0.028
(x)	359.876	0.013	(aq)	362.289	0.020
(y)	359.895	0.014	(ar)	362.356	
(z)	360.356	0.013	(as)	362.401	0.007
(aa)	360.407	0.019	(at)	363.180	
(ab)	360.440	0.017	(au)	363.446	
(ac)	360.455	0.017	(av)	363.553	

Nishikawa[9,10] as a result of transitions to other nearby excited states involving acoustic phonons.

We had earlier developed a model that explains both the magnitude and the distribution of the acceptor ground-state splitting caused by the isotopic disorder present in ^{nat}Si,[29] in order to explain an acceptor ground-state splitting which can be observed in acceptor-bound exciton spectra in ^{nat}Si. We computed the eigenvalues of the ground state for B, for different configurations of random distributions of isotopes around the lattice site, with an average composition corresponding to ^{nat}Si. The perturbation induced by the isotopes splits the fourfold degenerate eigenvalues of the acceptor ground state into Kramers doublets and shifts them randomly, leading to a broad distribution. This distribution of the B ground-state eigenvalues has been convoluted with the lines $1\Gamma_6$, $1\Gamma_7$, $2\Gamma_7$, $3\Gamma_6$, and $3\Gamma_7$ obtained from a ^{28}Si sample and is shown in Fig. 5 together with transitions in natural Si and isotopically pure ^{28}Si. The result is seen to be in excellent agreement with the spectrum observed in ^{nat}Si, showing that the inhomogeneous isotopic broadening of the infrared-absorption transitions can be accounted for with no adjustable parameters.

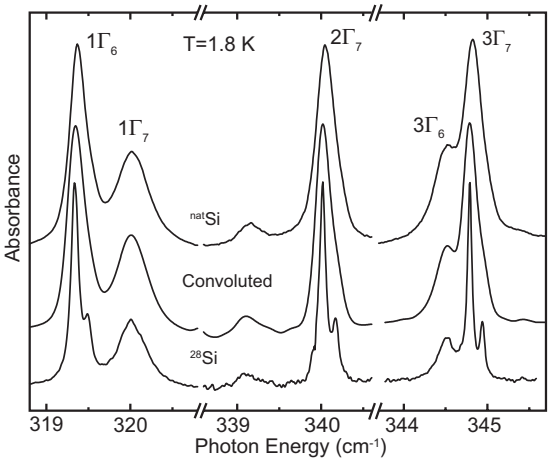

FIG. 5. Absorption lines $1\Gamma_6$, $1\Gamma_7$, $2\Gamma_7$, $3\Gamma_6$, and $3\Gamma_7$ of the B acceptor are compared between ^{nat}Si (top) and ^{28}Si (bottom). Lines $1\Gamma_6$, $2\Gamma_7$, and $3\Gamma_7$ are significantly narrower in ^{28}Si, revealing an identical doublet structure with a splitting of 0.154 cm^{-1} due to the difference in binding energy between ^{10}B and ^{11}B. The $1\Gamma_7$ transition is broad in both spectra, indicating the dominance of excited-state lifetime broadening for this state even in ^{nat}Si. The middle spectrum shows an excellent agreement between the ^{nat}Si spectrum and the ^{28}Si spectrum convoluted with the previously calculated isotopic broadening of the B ground state in ^{nat}Si (Ref. 29).

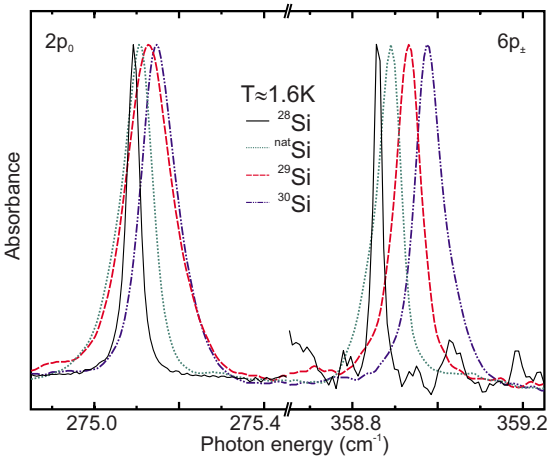

FIG. 6. (Color online) Shifts for two representative P transitions ($2p_0$ and $6p_\pm$) in ^{28}Si, ^{nat}Si, ^{29}Si, and ^{30}Si.

2. Line shapes

The phosphorus absorption lines exhibit tails in ^{nat}Si and ^{30}Si. In natural silicon the tail is toward the lower-energy end, in ^{30}Si it is on the high-energy side of the peak. The ^{28}Si lines do not show this asymmetry while the ^{29}Si absorption lines show broadening on both sides. Figure 6 clearly shows the effect, especially for the $2p_0$ line.

C. Binding-energy shifts

Figures 6 and 7 show the energies for two representative P and B transitions in ^{28}Si, ^{nat}Si, ^{29}Si, and ^{30}Si, respectively. The dependence of ϵ_0 and m^* on the isotopic mass scales the ground-state and excited-state binding energies by an identical factor,[12] and thus the largest shifts are observed for transitions to the highest-excited states. To obtain the actual isotope shift between ^{28}Si and ^{30}Si it was necessary to scale the energy of the ^{30}Si transition since the ^{30}Si sample has an enrichment of only 89.8% ^{30}Si. To obtain an appropriate scaling factor for the shift of the binding energy $\Delta E_B = E_B(^{28}\text{Si}) - E_B(^{30}\text{Si})$, we simply assume that the binding energy depends linearly on the average Si mass.

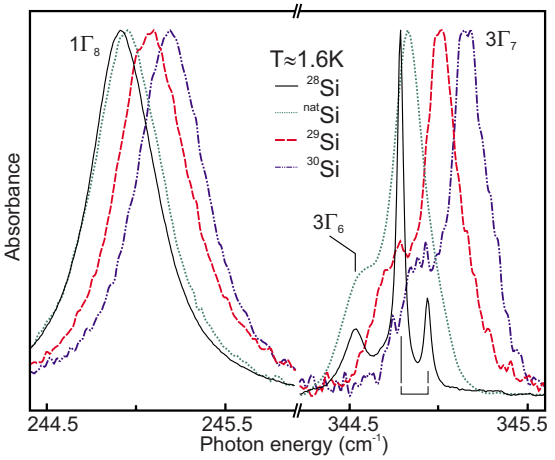

FIG. 7. (Color online) Shifts for two representative B transitions ($1\Gamma_8$ and $3\Gamma_7$) in ^{28}Si, ^{nat}Si, ^{29}Si, and ^{30}Si. While the $1\Gamma_8$ absorption line is dominated by lifetime broadening in all samples, the $3\Gamma_7$ transition reveals the ^{11}B/^{10}B splitting in ^{28}Si.

At the high-energy end of the spectrum the changes in the energy shift between ^{28}Si and ^{30}Si from line to line are very small, since the excited-state binding energies and their shifts with the average Si mass become small. This allows us to choose a high-lying absorption line with strong intensity, which shows essentially the full binding-energy shift of the ground state between pure ^{28}Si and pure ^{30}Si. For phosphorus we selected one of the sharpest features, the $6p_{\pm}$ transition. Scaling the measured shift we obtain the P ground-state binding-energy shift between pure ^{28}Si and pure ^{30}Si, $\Delta E_B=(-0.14\pm0.01)$ cm^{-1}. The $6p_{\pm}$ transition has a binding energy of only 1.08 meV versus 45.6 meV of the phosphorus ground state. In the case of boron we chose the highest-isolated line in the spectrum, the $3\Gamma_7$ transition. For ^{28}Si we use the energy of the ^{11}B component due to its high abundance. The resulting B ground-state binding-energy shift between pure ^{28}Si and pure ^{30}Si is then $\Delta E_B=(-0.41\pm0.02)$ cm^{-1}. $3\Gamma_7$ has an E_B of 2.41 meV versus 45.6 meV of the boron ground state. Hence the transition energies of both $6p_{\pm}$ and $3\Gamma_7$ can be considered close to the ionization energy. Table IV lists the experimentally determined energy shift for select transitions together with ΔE_B for P and B.

TABLE IV. Experimentally determined energy shifts for select transitions between ^{28}Si and ^{30}Si and the calculated shift of the binding energy $\Delta E_B=E_B(^{28}\text{Si})-E_B(^{30}\text{Si})$ for P and B between pure ^{28}Si and pure ^{30}Si (in cm^{-1}). ΔE_B has an error of ±0.01 for P and ±0.02 for B.

	P				B			
	$2p_{\pm}$	$3p_{\pm}$	$6p_{\pm}$	ΔE_B	$1\Gamma_8$	$1\Gamma_6$	$3\Gamma_7$	ΔE_B
ΔE	−0.10	−0.12	−0.13	−0.14	−0.26	−0.35	−0.38	−0.41

IV. CONCLUSION

We have shown improved spectra of the shallow impurities phosphorus and boron in natural silicon, ^{28}Si, ^{29}Si, and ^{30}Si. For phosphorus in ^{nat}Si we observe higher-excited states than reported previously. In ^{28}Si we show high-energy absorption transitions of phosphorus up to the $9f_{\pm}$ line. The observed FWHM is significantly narrower than in natural silicon. In the case of boron, we find strong evidence of the existence of many more highly-excited states than previously reported. We developed a way of identifying those transitions with the help of their boron isotope components. Many of these transitions are extremely sharp. They are the sharpest reported for shallow impurity absorption transitions in silicon. We also measure the binding-energy shift in samples with different host isotopic compositions for B and P and find that the ground-state binding-energy shift ΔE_B between pure ^{28}Si and pure ^{30}Si is smaller than previously estimated. These significant improvements were made possible by the use of greatly improved isotopically enriched silicon samples.

ACKNOWLEDGMENTS

We acknowledge NSERC for financial support, and thank B. Pajot for several useful discussions.

*thewalt@sfu.ca

[1] E. E. Haller, J. Appl. Phys. **77**, 2857 (1995).
[2] M. Cardona, Phys. Status Solidi B **220**, 5 (2000).
[3] V. G. Plekhanov, Semicond. Semimetals **68**, 23 (2001).
[4] A. D. Bulanov, G. G. Devyatych, A. V. Gusev, P. G. Sennikov, H.-J. Pohl, H. Riemann, H. Schilling, and P. Becker, Cryst. Res. Technol. **35**, 1023 (2000).
[5] P. Becker *et al.*, Meas. Sci. Technol. **17**, 1854 (2006).
[6] D. Karaiskaj, M. L. W. Thewalt, T. Ruf, M. Cardona, H.-J. Pohl, G. G. Deviatych, P. G. Sennikov, and H. Riemann, Phys. Rev. Lett. **86**, 6010 (2001).
[7] D. Karaiskaj, J. A. H. Stotz, T. Meyer, M. L. W. Thewalt, and M. Cardona, Phys. Rev. Lett. **90**, 186402 (2003).
[8] E. O. Kane, Phys. Rev. **119**, 40 (1960).
[9] K. Nishikawa and R. Barrie, Can. J. Phys. **41**, 1135 (1963).
[10] R. Barrie and K. Nishikawa, Can. J. Phys. **41**, 1823 (1963).
[11] N. Q. Vinh *et al.*, Proc. Natl. Acad. Sci. U.S.A. **105**, 10649 (2008).
[12] D. Karaiskaj, T. A. Meyer, M. L. W. Thewalt, and M. Cardona, Phys. Rev. B **68**, 121201(R) (2003).
[13] H. Kim, A. K. Ramdas, S. Rodriguez, and T. R. Anthony, Solid State Commun. **102**, 861 (1997).
[14] M. Cardona, Solid State Commun. **121**, 7 (2001).
[15] M. Steger *et al.*, in *Physics of Semiconductors: 28th International Conference on the Physics of Semiconductors*, AIP Conf. Proc. Vol. 893 (AIP, New York, 2007), pp. 231–232.

[16] A. Yang *et al.*, Phys. Rev. Lett. **97**, 227401 (2006).
[17] G. G. Devyatykh *et al.*, Dokl. Chem. **421**, 157 (2008).
[18] D. Karaiskaj, M. L. W. Thewalt, T. Ruf, M. Cardona, and M. Konuma, Solid State Commun. **123**, 87 (2002).
[19] A. N. Safonov, G. Davies, and E. C. Lightowlers, Phys. Rev. B **54**, 4409 (1996).
[20] C. Jagannath, Z. W. Grabowski, and A. K. Ramdas, Solid State Commun. **29**, 355 (1979).
[21] C. Jagannath, Z. W. Grabowski, and A. K. Ramdas, Phys. Rev. B **23**, 2082 (1981).
[22] B. Pajot, J. Kauppinen, and R. Anttila, Solid State Commun. **31**, 759 (1979).
[23] B. A. Andreev, E. B. Kozlov, and T. M. Lifshits, Mater. Sci. Forum **196-201**, 121 (1995).
[24] B. Pajot, G. Grossmann, M. Astier, and C. Naud, Solid State Commun. **54**, 57 (1985).
[25] R. A. Lewis, P. Fisher, and N. A. McLean, Aust. J. Phys. **47**, 329 (1994).
[26] A. Onton, P. Fisher, and A. K. Ramdas, Phys. Rev. **163**, 686 (1967).
[27] D. W. Fischer and J. J. Rome, Phys. Rev. B **27**, 4826 (1983).
[28] M. Steger *et al.*, Physica B **401-402**, 600 (2007).
[29] D. Karaiskaj, G. Kirczenow, M. L. W. Thewalt, R. Buczko, and M. Cardona, Phys. Rev. Lett. **90**, 016404 (2003).